bioRxiv preprint doi: https://doi.org/10.1101/286500; this version posted March 23, 2018. The copyright holder for this preprint (which was not certified by peer review) is the author/funder, who has granted bioRxiv a license to display the preprint in perpetuity. It is made available under aCC-BY-NC-ND 4.0 International license.

A mutation-independent approach via transcriptional upregulation of a disease modifier gene rescues muscular dystrophy *in vivo*

Dwi U. Kemaladewi[1,*], Prabhpreet S. Bassi[1,2,*], Kyle Lindsay[1], Steven Erwood[1,2], Ella Hyatt[1], Kara M. Place[1], Ryan Marks[1], Kinga I. Gawlik[3], Madeleine Durbeej[3], Evgueni A. Ivakine[1,**], Ronald D. Cohn[1,2,4,**]

[1]Program in Genetics and Genome Biology, the Hospital for Sick Children Research Institute, Toronto, Canada

[2]Department of Molecular Genetics, University of Toronto, Canada

[3]Unit of Muscle Biology, Department of Experimental Medical Science, Lund University, Lund, Sweden

[4]Department of Pediatrics, the Hospital for Sick Children, Toronto, Canada

*Co-first authors

**Co-corresponding authors

bioRxiv preprint doi: https://doi.org/10.1101/286500; this version posted March 23, 2018. The copyright holder for this preprint (which was not certified by peer review) is the author/funder, who has granted bioRxiv a license to display the preprint in perpetuity. It is made available under aCC-BY-NC-ND 4.0 International license.

Introductory paragraph

Identification of protective and/or pathogenic genetic modifiers provides important insight into the heterogeneity of disease presentations in individuals affected by neuromuscular disorders (NMDs), despite having well-defined pathogenic variants. Targeting modifier genes to improve disease phenotypes could be especially beneficial in cases where the causative genes are large, structurally complex and the mutations are heterogeneous. Here, we report a mutation-independent strategy to upregulate expression of a compensatory disease-modifying gene in Congenital Muscular Dystrophy type 1A (MDC1A) using a CRISPR/dCas9-based transcriptional activation system.

MDC1A is caused by nonfunctional Laminin α2, which compromises muscle fibers stability and axon myelination in peripheral nerves [1]. Transgenic overexpression of *Lama1*, encoding a structurally similar protein Laminin α1, ameliorates muscle wasting and paralysis in the MDC1A mouse models, demonstrating its role as a protective disease modifier [2]. Yet, upregulation of *Lama1* as a postnatal gene therapy is hampered by its large size, which exceeds the current genome packaging capacity of clinically relevant delivery vehicles such as adeno-associated viral vectors (AAVs).

In this study, we sought to upregulate *Lama1* using CRISPR/dCas9-based transcriptional activation system, comprised of catalytically inactive *S. aureus* Cas9 (dCas9) fused to VP64 transactivation domains and sgRNAs targeting the *Lama1* promoter. We first demonstrated robust upregulation of *Lama1* in myoblasts, and following AAV9-mediated intramuscular delivery, in skeletal muscles of dy^{2j}/dy^{2j} mouse model of MDC1A.

We therefore assessed whether systemic upregulation of *Lama1* would yield therapeutic benefits in dy^{2j}/dy^{2j} mice. When the intervention was started early in pre-symptomatic dy^{2j}/dy^{2j} mice, *Lama1* upregulation prevented muscle fibrosis and hindlimb paralysis. An important question for future therapeutic approaches for a variety of disorders concerns the therapeutic window and phenotypic reversibility. This is particularly true for muscular dystrophies as it has long been hypothesized that fibrotic changes in skeletal muscle represent an irreversible disease state that would impair any therapeutic intervention at advanced stages of the disease. Here, we demonstrate that dystrophic features and disease progression were significantly improved and partially reversed when the treatment was initiated in symptomatic 3-week old dy^{2j}/dy^{2j} mice with already-apparent hind limb paralysis and significant muscle fibrosis.

bioRxiv preprint doi: https://doi.org/10.1101/286500; this version posted March 23, 2018. The copyright holder for this preprint (which was not certified by peer review) is the author/funder, who has granted bioRxiv a license to display the preprint in perpetuity. It is made available under aCC-BY-NC-ND 4.0 International license.

Collectively, our data demonstrate the feasibility and therapeutic benefit of CRISPR/dCas9-mediated modulation of a disease modifier gene, which opens up an entirely new and mutation-independent treatment approach for all MDC1A patients. Moreover, this treatment strategy provides evidence that muscle fibrosis can be reversible, thus extending the therapeutic window for this disorder. Our data provide a proof-of-concept strategy that can be applied to a variety of disease modifier genes and a powerful therapeutic approach for various inherited and acquired diseases.

bioRxiv preprint doi: https://doi.org/10.1101/286500; this version posted March 23, 2018. The copyright holder for this preprint (which was not certified by peer review) is the author/funder, who has granted bioRxiv a license to display the preprint in perpetuity. It is made available under aCC-BY-NC-ND 4.0 International license.

Congenital muscular dystrophy 1A (MDC1A) is an autosomal recessive neuromuscular disease associated with a high degree of morbidity and mortality in early childhood [1]. It is caused by mutations in the *LAMA2* gene encoding Laminin α2 chain (LAMA2), which interacts with the β1 and γ1 chains to form the heterotrimer Laminin-211, an extracellular matrix protein (reviewed in [3]). Laminin-211 interacts with α-dystroglycan and α7β1 integrin in skeletal muscle and Schwann cells, providing the necessary roles such as survival and stability of myotubes, as well as proper neurite growth, axon myelination and migration of Schwann cells. Lack of Laminin-211 in MDC1A causes degeneration of skeletal muscle and impaired Schwann cell differentiation, resulting in a cascade of secondary events including apoptosis/necrosis of muscle fibers, inflammation, and fibrosis, which ultimately precipitate the disease. Despite significant advances in our understanding of MDC1A pathophysiology, currently, there is no cure.

Due to the genetic nature of the disease, gene therapy is a promising treatment option for MDC1A. The large size of *LAMA2* transcript, however, presents a challenge with respect to gene delivery. We have recently overcome this challenge by using CRISPR/Cas9 technology to correct a mutation in *Lama2* gene *in vivo* [4]. We focused on dy^{2j}/dy^{2j} mouse model, which harbors a splice site mutation in *Lama2* causing spontaneous exon skipping and truncation of N-terminal domain of the protein [5]. We developed an exon inclusion strategy to correct the splice mutation, leading to restoration of full-length Lama2. This study established the first direct correction of the primary genetic defect underlying MDC1A in an *in vivo* model.

To date, there are over 350 reported pathogenic nonsense-, missense-, splice site- and deletion mutations in the *LAMA2* gene. Given the variety of MDC1A-causing genomic alterations, CRISPR/Cas9-mediated gene editing strategies would require design and thorough analysis of multiple sgRNAs specific for each individual mutation. Moreover, safety concerns regarding CRISPR/Cas9's potential mutagenic nature and the presence of off-target effects after gene editing remain, which together may prove to be challenging from a safety and regulatory point-of-view. In contrast, the attenuation of disease pathogenicity by targeted modulation of disease modifier gene expression would be a potentially safer alternative and beneficial to all individuals with MDC1A.

One of the strongest reported disease modifiers for MDC1A is Laminin-α1 protein, which is structurally similar to Laminin-α2 (**Fig. 1a**). However, Laminin-α1 is not expressed in skeletal muscles or Schwann cells. A series of studies previously demonstrated that transgenic expression of *Lama1*, encoding Laminin-α1, rescued both myopathy and

bioRxiv preprint doi: https://doi.org/10.1101/286500; this version posted March 23, 2018. The copyright holder for this preprint (which was not certified by peer review) is the author/funder, who has granted bioRxiv a license to display the preprint in perpetuity. It is made available under aCC-BY-NC-ND 4.0 International license.

peripheral neuropathy in *dy^{2j}/dy^{2j}* [6] and *dy^{3K}/dy^{3K}* [2,7-10]; the latter also showed increased lifespan. Although these studies firmly established compensatory function of Laminin-α1 in MDC1A, utilization of this modifier as a postnatal gene therapy is hampered by the size of *Lama1* cDNA, which exceeds the 4.7 kb packaging capacity of AAV vectors. Advances in CRISPR/Cas9 technologies have provided opportunities for regulating gene expression and creating epigenetic alterations without introducing DNA double-strand breaks (DSBs); commonly termed CRISPR transcriptional activation/inhibition system. The strategy utilizes nuclease-deficient Cas9 (dCas9), which is unable to cleave DNA due to mutations within the nuclease domains, but still retains the ability to specifically bind to DNA when guided by a single guide RNA (sgRNA) [11,12]. Using the originally described *S. pyogenes* (*Sp*) dCas9 fused to multiple copies of the VP16 transcriptional activator, our group and others have demonstrated utilization of the CRISPR/dCas9 system to upregulate expression of modifier genes *in vitro* [11-14]. A major challenge for *in vivo* applications lies in the large size of *Sp*dCas9 and its transcriptional activator fusion derivatives that exceed AAV genome packaging capacity. To accommodate this limitation, we sought to adapt the transcriptional upregulation system and utilize a significantly smaller Cas9 protein derived from *S. aureus* (*Sa*)[15] to upregulate MDC1A modifier *Lama1*. We hypothesized that CRISPR/dCas9-mediated transcriptional upregulation of *Lama1* would be sufficient to compensate for the lack of *Lama2* and ameliorate disease phenotypes in *dy^{2j}/dy^{2j}* mice.

First, we mutagenized *Sa*Cas9 endonuclease catalytic residues (D10A, N580A) to create *Sa*dCas9 and then fused it to transcriptional activators VP64 (four copies of VP16) on both N- and C-termini (**Fig. S1**). We tested the ability of the system, denoted as *Sa*dCas9-2xVP64, to upregulate the expression of minCMV-driven *tdTomato* gene in 293T cells [16]. In the absence of the *Sa*dCas9-2xVP64, the expression of *tdTomato* was undetectable due to the low baseline activity of minCMV promoter (**Fig. S1a, b**). In the presence of *Sa*dCas9-2xVP64 in combination with an sgRNA targeting the minCMV locus, we observed high *tdTomato* fluorescence signal (**Fig. S1c, d**), indicating the general applicability of this system to modulate expression of a gene of interest. Subsequently, we tailored the system to upregulate *Lama1* expression and designed five sgRNAs, denoted as g1 to g5, within the 500 nucleotides region immediately upstream of the *Lama1* transcription start site (**Figs. 1b, c**). When co-expressed with *Sa*dCas9-VP64 in C2C12 murine myoblasts, 3 out of 5 sgRNAs, namely g1, g2, and g5 consistently induced significant increase of *Lama1* transcript expression (**Figs. 1d, e**).

bioRxiv preprint doi: https://doi.org/10.1101/286500; this version posted March 23, 2018. The copyright holder for this preprint (which was not certified by peer review) is the author/funder, who has granted bioRxiv a license to display the preprint in perpetuity. It is made available under aCC-BY-NC-ND 4.0 International license.

Although all sgRNAs were designed to target a chromatin-accessible region derived from DNAse1 hypersensitivity- and assay for transposase-accessible chromatin (ATAC-Seq) sites (**Fig. 1b**), g3 and g4 failed to increase expression of *Lama1* above the basal level. This corroborates previously reported findings that chromatin accessibility is not a reliable predictor of successful gene activation [12,17,18]. Nonetheless, the sgRNA closest to the transcription start site, g1, and the combination of the three most optimum sgRNAs (g1, g2, g5) resulted in a robust increase in Lama1 protein expression in dy^{2j}/dy^{2j}-derived myoblasts (**Figs. 1f, 1g**), warranting further investigation *in vivo*.

We then treated 3-week-old dy^{2j}/dy^{2j} mice with an AAV9 carrying FLAG-tagged *Sa*dCas9-2xVP64 in the absence of sgRNA (no guide) or with g1 (single guide) or a combination of g1, g2 and g5 (three guides) (**Fig. 2a**). Each mouse received a single intramuscular injection of the AAV9 cocktail of 7.5×10^{11} vector genomes in the right *tibialis anterior* (TA) and was sacrificed 4 weeks post injection. FLAG expression was detected by Western blot in all *Sa*dCas9-2xVP64-injected right TA muscles, however, only those injected with guide-containing constructs showed Lama1 upregulation (**Fig. 2b**). Similarly, immunofluorescence staining revealed sarcolemmal expression of Lama1 (**Fig. 2c**, upper), indicating proper protein localization. Furthermore, H&E staining exhibited considerably improved muscle architecture (**Fig. 2c**, lower) in the single- and three guide treatment groups, as compared to the no guide controls.

Next, we sought to investigate whether upregulation of *Lama1* could be achieved systemically *in vivo* and, if administered into pre-symptomatic neonatal dy^{2j}/dy^{2j} mice, would prevent the manifestation of dystrophic pathophysiology and paralysis. AAV9 particles carrying either no guide or a combination of three guides were injected into the temporal vein of 2-day-old (P2) dy^{2j}/dy^{2j} mice (**Fig. 3a**). Seven weeks post injection, the animals that received the three guides treatment showed an absence of classical hindlimb contracture, as opposed to the control group (**Fig. 3b; Supplementary videos 1** and **2**). Western blot, immunofluorescence and H&E staining of TA and gastrocnemius muscles demonstrated robust expression of Lama1 on the sarcolemmal membrane (**Fig. 3c, 3d**), leading to ~50% reduction of fibrosis (**Figs. 3e**, **3f, S2**).

We next examined the ability of *Lama1* upregulation to reverse established muscular and peripheral nerve dysfunctions by initiating the treatment at 3-weeks of age, when paralysis was already apparent. We injected the dy^{2j}/dy^{2j} mice with increasing doses of AAV9 from 7.5×10^{11} to 3×10^{12} vector genomes via tail vein injection (**Figs. S3, 4a**). Expression of Lama1 was achieved in all doses tested (**Fig. S3**), however, the highest

bioRxiv preprint doi: https://doi.org/10.1101/286500; this version posted March 23, 2018. The copyright holder for this preprint (which was not certified by peer review) is the author/funder, who has granted bioRxiv a license to display the preprint in perpetuity. It is made available under aCC-BY-NC-ND 4.0 International license.

dose of $3x10^{12}$ vector genomes resulted in the most robust Lama1-positive muscle fibers (**Fig. 4b**, **Fig. S3**). Further analyses of the treated mice revealed strong Lama1 expression by Western blot (**Fig. 4c**), significant improvement in muscle histopathology (**Fig. 4d**) and approximately 50% reduction in the fibrotic area (**Fig. 4e**) compared to the no guide control group.

In addition to the skeletal muscle, Laminin α2-deficiency also affects peripheral nervous system. Previous studies showed that the peripheral neuropathy phenotypes are alleviated exclusively in transgenic mice that overexpress Lama1 not only in the skeletal muscle, but also in the nerves [7]. We observed expression of Lama1 in the endoneurium of sciatic nerves in the treated mice (**Fig. 4f**). Furthermore, specific tetanic force, which measures the aggregate torque produced by the dorsi flexor muscles, was also improved upon Lama1 upregulation (**Fig. 4g**). In line with this finding, the degree of paralysis in the hind limbs and mobility of the treated mice were markedly improved (**Fig. 4h; Supplementary videos 3, 4**), indicating the robustness and therapeutic promise of CRISPR/dCas9-mediated Lama1 upregulation for the treatment of MDC1A. Taken together, our results provide strong evidence for partial reversal of dystrophic feature in skeletal muscle and peripheral neuropathy in dy^{2j}/dy^{2j} mouse model of MDC1A, which ultimately halts progression of the disease.

bioRxiv preprint doi: https://doi.org/10.1101/286500; this version posted March 23, 2018. The copyright holder for this preprint (which was not certified by peer review) is the author/funder, who has granted bioRxiv a license to display the preprint in perpetuity. It is made available under aCC-BY-NC-ND 4.0 International license.

One hurdle in developing a therapy for MDC1A is that the extent of heterogeneity of mutations often leads to variable disease severity and progression. Therefore, there is an urgent need to develop a universal, mutation-independent strategy that provides a treatment approach for all patients with MDC1A. Our study establishes a framework in which CRISPR/dCas9 transcriptional upregulation of a disease modifier gene, such as *Lama1,* ameliorates disease symptoms *in vivo* and has the potential to be applied to all MDC1A patients, irrespective of their mutations.

Advances have been made towards elucidating MDC1A pathogenesis due to the availability of several mouse models with absent or reduced *Lama2* expression. Yet, a crucial question facing therapeutic development and clinical trials in MDC1A is the reversibility of symptoms such as muscle fibrosis and significant paralysis. This issue, while critically important for therapeutic development, is difficult to address in patients [19], but the ability to modify gene expression in postnatal animals allowed us to address this question and investigate the therapeutic window of intervention.

We have previously demonstrated that an early intervention using CRISPR/Cas9-mediated correction of a splicing defect resulted in robust Lama2 restoration and prevention of disease manifestation [4]. Here we showed that upregulation of *Lama1*, when initiated at pre-disease-onset, leads to similar prevention. Importantly, when the therapeutic intervention was initiated at older age, significant rescue of the phenotypes was attainable, indicating that post-symptomatic treatment provides a significant benefit in the dy^{2j}/dy^{2j} mouse model.

In addition to *Lama1* upregulation described in this study, a number of disease modifying strategies are currently being explored in MDC1A animal models, such as treatment with miniaturized agrin [20-22] and laminin-α1 LN-domain nidogen-1 (αLNNd) [23-25]. While the efficacy of αLNNd has only been explored in transgenic mice, AAV-mediated delivery of mini agrin has been shown to normalize most histopathological parameters in skeletal muscle, and improve myelination and regeneration of Schwann cells of the peripheral nerves [20,22]. Despite the observed phenotypic improvement, the mini agrin-treated mice still have a lower survival rate compared to wild-type animals expressing full-length agrin, suggesting the potential shortcoming of the shortened version of agrin, which may be overcome by its full-length form in native glycosylation state [23]. Our approach in combining the CRISPR/dCas9-mediated transcriptional upregulation and AAV9 as a delivery vehicle can be translated to many other disease modifiers, such as agrin, as

bioRxiv preprint doi: https://doi.org/10.1101/286500; this version posted March 23, 2018. The copyright holder for this preprint (which was not certified by peer review) is the author/funder, who has granted bioRxiv a license to display the preprint in perpetuity. It is made available under aCC-BY-NC-ND 4.0 International license.

well as conditions where modulation of disease modifiers is required within skeletal muscles and peripheral nerves.

In fact, neuromuscular disorders have provided excellent examples to demonstrate the role of disease modifiers (recently reviewed in [26]). Beyond MDC1A, several studies have demonstrated that upregulation of *Lama1* stabilizes the sarcolemmal membrane in dystrophin-deficient mouse models [27]. The most advanced approach is via delivery of Laminin-111 protein, although the efficacy remains low and the need to produce a large amount of bioactive protein is challenging [27]. In addition, the utilization of CRISPR/dCas9 system to upregulate Lama1 in *mdx* mice has been achieved locally via electroporation, which is not easily translatable into clinical settings [28]. Our strategy of employing AAV-mediated *S. aureus* dCas9 to upregulate *Lama1 in vivo* may be tested further as a potential therapy in the context of Duchenne muscular dystrophy.

In addition to overcoming the cDNA size challenge for AAV9 packaging, our approach may also be superior in several cases where gene delivery does not lead to a complete rescue due to the use of mini promoters and/or minimal regulatory elements [29]. The CRISPR/dCas9-mediated transcriptional modulation acts directly on the endogenous locus, thereby maximizing the chance of successful upregulation and correct temporal and spatial expression patterns.

A very recent study by Liao *et al* described utilization of the CRISPR/Cas9 system to recruit MCP:P65:HSF1 transcriptional activation complex to induce expression of target genes in skeletal muscle, kidney and liver tissues [18]. This resulted in phenotypic augmentation such as enhanced muscle mass and substantial improvement in disease pathophysiology, thereby highlighting the feasibility of using CRISPR/dCas9-mediated transcriptional activation as a possible therapeutic modality. However, their study relied almost exclusively on a Cas9-expressing transgenic mouse model or local intramuscular treatments, and therefore it is difficult to extrapolate the efficacy of this strategy to disease-relevant models. In contrast, we successfully demonstrated robust upregulation of Lama1 after systemic delivery of therapeutic components in a relevant mouse model of disease that does not constitutively express Cas9.

Finally, the modular nature of the CRISPR/dCas9 system can be utilized to not only to upregulate, but also to downregulate target gene expression. The latter can be achieved by coupling dCas9 with transcriptional repressor such as Kruppel-associated box (KRAB) [17,30]. A very recent study described that following sarcolemmal injury, the muscle membrane resealing process is greatly improved upon the deletion of Osteopontin,

bioRxiv preprint doi: https://doi.org/10.1101/286500; this version posted March 23, 2018. The copyright holder for this preprint (which was not certified by peer review) is the author/funder, who has granted bioRxiv a license to display the preprint in perpetuity. It is made available under aCC-BY-NC-ND 4.0 International license.

which acts in a concerted fashion with protective modifiers such as Latent TGF-β binding protein (LTBP4) and Annexins 1 and 6 [31,32]. The combinatorial effects of such modifiers, whether they are additive, synergistic or even opposing in action, represent a new paradigm for lessening disease phenotypes. A foreseeable application of CRISPR/dCas9-mediated modulation in the future is in the upregulation of protective disease modifier genes, such as Lama1 or LTBP4, with concurrent downregulation of detrimental genes, such as Osteopontin, providing a combinatorial therapeutic approach. In summary, our study establishes a framework to utilize CRISPR/dCas9 to modulate gene expression of disease modifiers that should be considered as a mutation-independent therapeutic strategy not only to MDC1A, but also to various other inherited and acquired diseases.

bioRxiv preprint doi: https://doi.org/10.1101/286500; this version posted March 23, 2018. The copyright holder for this preprint (which was not certified by peer review) is the author/funder, who has granted bioRxiv a license to display the preprint in perpetuity. It is made available under aCC-BY-NC-ND 4.0 International license.

Methods

Engineering of Activation *S. aureus* dCas9, Cloning and Virus Production

A fragment containing a catalytically inactive *SaCas9* coupled to two flanking VP64 transactivator domains was synthesized by BioBasic Canada and cloned into pX601 (Addgene 61591) using AgeI and EcoRI directional cloning to generate 3XFLAG-VP64-SadCas9 (D10A/N580A)-NLS-VP64 plasmid (**Fig. S4**). Each sgRNA **(Supplementary Table 1)** was subsequently introduced using BsaI directional cloning.

VP64-dCas9, VP64-dCas9 sgRNA 1 and VP64-dCas9 sgRNA 123 plasmids were packaged into AAV9 vectors by Vigene Biosciences as previously described [3]. Injection solutions were comprised of either $7.5x10^{11}$, $1.5x10^{12}$ or $3.0x10^{12}$ viral genome/AAV9 and brought up to 50uL with 1xPBS (Gibco).

Cell Culture

Primary myoblasts were isolated from the Extensor Digitorum Longus (EDL) Muscle of dy^{2J}/dy^{2J} mice, as previously described [33] and maintained in DMEM supplemented with 1% chicken embryo extract (GeminiBioscience), 10% horse serum, 1% penicillin/streptomycin and 1% L-glutamine (all from Gibco, unless indicated otherwise). HEK293 and C2C12 cells where maintained in DMEM supplemented with 10% FBS, 1% penicillin/streptomycin and 1% L-glutamine (all from Gibco). All cells were maintained at 37°C with 5% CO_2.

Transfection of HEK293T cells was performed as previously described[2]. C2C12 and dy^{2J}/dy^{2J} cells were transfected in 12-well plates using the Neon Transfection System (Invitrogen). 400,000 cells were electroporated with 1.5ug of DNA utilizing optimization program 16 (pulse voltage: 1400V, pulse width: 20ms, pulse number: 2). Cells were grown for 72 hours, after which RNA or protein was subsequently collected for protein analysis and guide screening.

RNA isolation, guide screening and RT-PCR

RNA was isolated from cultured cells and mouse tissue sections, and cDNA synthesis was performed as previously described[3]. PCR amplification was utilized to assess the efficiency of each guide in upregulating *Lama1* expression using a primer in *Lama1* exon 55 (RDC 1919) and a second primer spanning the junction of exons 55 and 56 (RDC 1920). Sequences are listed in **Supplementary Table 2**.

bioRxiv preprint doi: https://doi.org/10.1101/286500; this version posted March 23, 2018. The copyright holder for this preprint (which was not certified by peer review) is the author/funder, who has granted bioRxiv a license to display the preprint in perpetuity. It is made available under aCC-BY-NC-ND 4.0 International license.

qPCR utilizing Fast SYBR green Master Mix (Qiagen) on a Step One Plus Real Time PCR (Applied Biosystems) was performed. *Lama1* expression was analyzed using a primer in *Lama1* exon 55 (RDC 1919) and one spanning the junction of exons 55 and 56 (RDC 1920). Primers against endogenous Gapdh (RDC 345 and 346) were used as an internal control. ΔΔCt was analyzed to assess fold changes between treated and untreated samples.

Protein Isolation and western blot

Protein was isolated from dy^{2J}/dy^{2J}, and C2C12 cells by adding 150uL of a 1:1 part solution of RIPA homogenizing buffer (50-mM Tris HCl pH 7.4, 150-nM NaCl, 1-mM EDTA) and RIPA double-detergent buffer (2% deoxycholate, 2% NP40, 2% Triton X-100 in RIPA homogenizing buffer) supplemented with protease-inhibitor cocktail (Roche). Cells were subsequently scraped from the bottom of each well, collected and incubated on ice for 30 min. Cells then centrifuged at 12000xg for 15 min at 4^{o}C and the supernatant was collected and stored at -80^{o}C. Protein from mouse tissue sections was collected as previously described[3]. Whole protein concentration was measured using Pierce BCA protein assay kit according to the manufacturer's protocol (Thermo Fisher Scientific). Western blot was performed as previously described[3]. Primary antibodies used were rabbit Anti-LNα1 E3 (a gift from Dr. Peter Yurchenco, 0.6 µg/ml), mouse monoclonal M2 anti-Flag (Sigma Aldrich F1804, 1:1000) and rabbit polyclonal anti-GAPDH (Santa Cruz sc-25778, 1:5000).

Immunofluorescence and H&E staining

Antibodies used for immunofluorescence staining were rat anti-200 LNα1 (Durbeej Laboratory, 1:20), mouse anti-NF-H (Biolegend SMI 31, 1:1000), goat polyclonal anti-rat Alexa Fluor 555 (Thermo Fisher Scientific, 1:250) and goat polyclonal anti-mouse Alexa Fluor 488 (Thermo fisher Scientific, 1:250). H&E staining was performed as previously described [4]. Both immunofluorescence and H&E slides were scanned with the 3Dhistech Pannoramic 250 Flash II digital scanner and analyzed with CaseViewer software. Morphometric analysis was performed as previously described [4].

Animal Studies and Functional tests

dy^{2j}/dy^{2j} mice were purchased from the Jackson Laboratory and maintained in the Toronto Center for Phenogenomics. All animal experiments were performed according to

bioRxiv preprint doi: https://doi.org/10.1101/286500; this version posted March 23, 2018. The copyright holder for this preprint (which was not certified by peer review) is the author/funder, who has granted bioRxiv a license to display the preprint in perpetuity. It is made available under aCC-BY-NC-ND 4.0 International license.

Animal Use Protocol number 16-0234H. Intramuscular and temporal vein injections were preformed as previously described [4]. Systemic administration experiments were performed on 3-week-old *dy*^{2j}/*dy*^{2j} mice through tail vein injection. All functional tests were performed as previously described [4].

Statistical Analysis

GraphPad Prism (GraphPad software) was utilized to preform all statistical analyses. Two-tailed Student' t-tests to evaluate statistical significance between two groups was preformed. Significance was considered to be $P < 0.05$.

Data availability

The authors declare that the main data supporting the findings of this study are available within the article and its Supplementary Information files. Extra data are available from the corresponding authors upon request.

Acknowledgements

We thank Dr. Peter Yurchenco (Rutgers, The State University of New Jersey, USA) for providing critical reagents and scientific input in this study, Chris Rand (Aurora Scientific) for assistance with contractile assay and the Toronto Center for Phenogenomics staff for mouse husbandry and colony maintenance. The Cohn lab members are gratefully acknowledged for the technical support and critical input in this study.
This work was supported by AFM-Telethon postdoctoral fellowship, Cure CMD, Muscular Dystrophy Association Development Grant (to D.U.K), Rare Disease Foundation Microgrant Program (to P.S.B. and S.E.), CIHR Summer Studentship (to R.M.), Natural Sciences and Engineering Research Council of Canada, Canadian Institute for Health Research, SickKids Foundation and R.S. McLaughlin Foundation Chair in Pediatrics (to R.D.C).

Author contributions

D.U.K., P.S.B., E.I., R.D.C. conceived the study and analyzed data, D.U.K., P.S.B., K.L., S.E., E.H., K.M.P., R.M. performed the experiments, K.G., M.D. provided critical reagents, D.U.K., E.I., R.D.C. supervised the study, D.U.K. wrote the manuscript with inputs from the other authors. All authors provided feedback and agreed on the final manuscript.

bioRxiv preprint doi: https://doi.org/10.1101/286500; this version posted March 23, 2018. The copyright holder for this preprint (which was not certified by peer review) is the author/funder, who has granted bioRxiv a license to display the preprint in perpetuity. It is made available under aCC-BY-NC-ND 4.0 International license.

bioRxiv preprint doi: https://doi.org/10.1101/286500; this version posted March 23, 2018. The copyright holder for this preprint (which was not certified by peer review) is the author/funder, who has granted bioRxiv a license to display the preprint in perpetuity. It is made available under aCC-BY-NC-ND 4.0 International license.

Figure legends

Fig. 1. *Sa*dCas9-2xVP64-mediated upregulation of *Lama1 in vitro*. (**a**) Lama1 and Lama2 protein domain alignment. Total amino acid (aa) and percentage similarity between each domain are indicated. (**b**) Analyses of Lama1 proximal promoter. Five sgRNAs (g1-g5) were designed in the proximal promoter region of Lama1 immediately upstream of the transcription start site (TSS), as indicated by CAGE tags (red). Chromatin accessibility in skeletal muscle tissue and cells (retrieved using Digital DNase footprinting and ATAC-Seq) are shown in blue. Data were plotted according to positions from the UCSC Genome Browser. (**c**) Positions of the five sgRNAs relative to *Lama1* TSS. Arrowheads indicate the direction of each sgRNA. Sequences of each sgRNA (red) are immediately downstream (5') of *Sa* PAM sequences (NNGRRT) (in blue). ATG indicates translation start site. (**d-e**) C2C12 myoblasts were transfected with a plasmid containing *Sa*dCas9-2xVP64 and the corresponding sgRNA(s) targeting *Lama1*, and 72 hours post-transfection, analyzed by (**d**) RT-PCR and (**e**) qRT-PCR. Single and combination of optimal sgRNAs were transfected into dy^{2j}/dy^{2j} myoblasts and Lama1 protein expression was assessed by Western blot (**f**). FLAG expression serves as transfection control and used to (**g**) normalize Lama1 upregulation by densitometry analysis. Data are presented as mean ± standard deviation from at least three independent experiments. Statistical analysis was performed using Student's *t*-test. $^{**}P<0.01$.

Fig. 2. Upregulation of Lama1 in *tibialis anterior* (TA) muscles of dy^{2j}/dy^{2j} mice following intramuscular administration. (**a**) Right TA muscles of three weeks old dy^{2j}/dy^{2j} mice were injected with AAV9-carrying no guide (n=4), single guide (n=4) or three guides (n=4) ($7.5x10^{11}$ vector genome each). In the three-guides approach, the vectors are split into two. ITR: Inverted Terminal Repeats. CMV and U6 promoters are depicted in arrows. Left TA muscles serve as control. (**b**) Western blot analysis on Lama1, FLAG-tagged *Sa*dCas9, and Gapdh expression. (**c**) Immunofluorescence (upper) and H&E (lower) stainings on cross-sections of right TA muscles from each treatment group. Scale bar: 50 µm. Representative images from one animal per treatment group are shown.

bioRxiv preprint doi: https://doi.org/10.1101/286500; this version posted March 23, 2018. The copyright holder for this preprint (which was not certified by peer review) is the author/funder, who has granted bioRxiv a license to display the preprint in perpetuity. It is made available under aCC-BY-NC-ND 4.0 International license.

Fig. 3. Early intervention to upregulate Lama1 prevents disease progression in *dy^{2j}/dy^{2j}* mice. (**a**) Two days old neonatal *dy^{2j}/dy^{2j}* mice were injected with AAV9 carrying no guide (n=3) or three guides (n=4) via temporal vein and sacrificed 7 weeks later. (**b**) Photographs of *dy^{2j}/dy^{2j}* from both treatment groups prior to sacrificing. Note the difference in hindlimb contractures. Lama1 expression was analyzed by (**c**) western blot and (**d**) immunofluorescence staining, and general histopathology was evaluated by (**e**) H&E staining. The muscle groups analyzed are indicated on each panel, except on (**c**), which shows tibialis anterior (TA) muscles. Scale bars: 100 µm (**d**), 200 µm (**e**). (**f**) The percentage of fibrosis from gastrocnemius (upper) and TA (lower) muscles are calculated and presented as mean ± standard deviation. Statistical analysis was performed using Student's *t*-test. **P*<0.05.

Fig. 4. Upregulation of Lama1 in older *dy^{2j}/dy^{2j}* mice slows down disease progression. (**a**) Three weeks old *dy^{2j}/dy^{2j}* mice were injected with AAV9 carrying no guide (n=5) or three guides (n=6) via tail vein and sacrificed four weeks later. (**b**) Immunofluorescence staining and (**c**) Western blot to analyze Lama1 expression and (**d**) H&E staining to (**e**) quantify fibrosis were performed on gastrocnemius muscles. (**f**) Sciatic nerves were stained for Lama1 (red) and Neurofilament H (green). Nuclei were counterstained by DAPI (blue). Higher magnification images from the dotted area are shown. (**g**) Specific tetanic force measured prior to sacrificing the mice. (**h**) Photographs of *dy^{2j}/dy^{2j}* mouse injected with AAV carrying no guide displaying a typical joint contracture in the hindlimbs, compared to treated *dy^{2j}/dy^{2j}* showing the near-normal hindlimb phenotype and stand-up ability. Scale bars: 100 µm (**b**), 50 µm (**d**), and 200 µm (**f**). Data are presented as mean ± standard deviation. Statistical analysis was performed using Student's *t*-test. **P*<0.05. ***P*<0.01.

Supplementary Figures, Tables and Videos

Fig. S1. ***Sa*dCas9-2xVP64 enhances expression of minCMV-driven *tdTomato in vitro*.** HEK293T was transfected with (**a**,**b**) a plasmid containing minCMV-driven *tdTomato* gene only, or (**c**,**d**) in combination with a plasmid containing *Sa*dCas9-2xVP64 and a sgRNA targeting the minCMV promoter. (**b**,**d**) Cells were imaged for *tdTomato* expression by fluorescent microscopy. Scale bar: 50 µm.

bioRxiv preprint doi: https://doi.org/10.1101/286500; this version posted March 23, 2018. The copyright holder for this preprint (which was not certified by peer review) is the author/funder, who has granted bioRxiv a license to display the preprint in perpetuity. It is made available under aCC-BY-NC-ND 4.0 International license.

Fig. S2. Expression of Lama1 and muscle architecture following early intervention in neonatal *dy^{2j}/dy^{2j}* mice. Lower magnification of immunofluorescence and H&E staining images of Fig. 3 in the main manuscript.

Fig. S3. Dose-dependent upregulation of Lama1 after systemic administration. Three-weeks old *dy^{2j}/dy^{2j}* mice were injected systemically with different doses of AAV9: 7.5x10^{11}, 1.5x10^{12}, or 3x10^{12} vector genome via tail vein. TA muscles isolated four weeks later were stained for Lama1 expression. Asterisks indicate Lama1-positive fibers in the low dose cohort. Scale bar: 100 µm.

Fig. S4. *Sa*dCas9-VP64 transcriptional activator plasmid.
Different domains are annotated accordingly. Amino acids encoding *Sa*dCas9 are in bold and italic, and the mutated residues D10A and N580A are indicated in red asterisk (*). NLS: Nuclear localization signal.

Table S1. sgRNA sequences used in this study

Table S2. Primers used in this study

Video S1. Phenotype of control *dy^{2j}/dy^{2j}* mouse following early intervention.
The *dy^{2j}/dy^{2j}* mouse was injected with AAV9 containing *Sa*dCas9-2xVP64 (no guide) at P2 (pre-symptomatic stage) via temporal vein and video was taken at the age of 7-week old. Hind limb paralysis, contracture and kyphosis resulting from lack of functional *Lama2* and compensatory *Lama1* are apparent.

Video S2. Phenotype of treated *dy^{2j}/dy^{2j}* mouse following early intervention.
The *dy^{2j}/dy^{2j}* mouse was injected with AAV9 containing *Sa*dCas9-2xVP64 and sgRNAs targeting *Lama1* proximal promoter (three guides) at P2 (pre-symptomatic stage) via temporal vein and video was taken at the age of 7-week old. Upregulation of compensatory *Lama1* expression ameliorates the hind limb paralysis, contracture and kyphosis.

Video S3. Phenotype of control *dy^{2j}/dy^{2j}* mouse following intervention at symptomatic stage.
The *dy^{2j}/dy^{2j}* mouse was injected with AAV9 containing *Sa*dCas9-2xVP64 (no guide) at 3-week old (pre-symptomatic stage) via tail vein. Video was taken at the age of 7-week

bioRxiv preprint doi: https://doi.org/10.1101/286500; this version posted March 23, 2018. The copyright holder for this preprint (which was not certified by peer review) is the author/funder, who has granted bioRxiv a license to display the preprint in perpetuity. It is made available under aCC-BY-NC-ND 4.0 International license.

old. Hind limb paralysis, contracture and kyphosis resulting from lack of functional *Lama2* and compensatory *Lama1* are apparent.

Video S4. Phenotype of treated *dy^{2j}/dy^{2j}* mouse following intervention at symptomatic stage.

The *dy^{2j}/dy^{2j}* mouse was injected with AAV9 containing *Sa*dCas9-2xVP64 and sgRNAs targeting *Lama1* proximal promoter (three guides) at 3-week old (pre-symptomatic stage) via tail vein. Video was taken at the age of 7-week old. Dystrophic features and disease progression were significantly improved and partially reversed following upregulation of *Lama1*.

References

1. Dowling, J. J., H, D. G., Cohn, R. D., Campbell, C. *American journal of medical genetics. Part A* 2017.
2. Gawlik, K., Miyagoe-Suzuki, Y., Ekblom, P., Takeda, S., Durbeej, M. *Human molecular genetics* 13:16. 2004.
3. Yurchenco, P. D., McKee, K. K., Reinhard, J. R., Ruegg, M. A. *Matrix biology : journal of the International Society for Matrix Biology* 2017.
4. Kemaladewi, D. U., Maino, E., Hyatt, E., Hou, H., Ding, M., Place, K. M., Zhu, X., Bassi, P., Baghestani, Z., Deshwar, A. G., Merico, D., Xiong, H. Y., Frey, B. J., Wilson, M. D., Ivakine, E. A., Cohn, R. D. *Nat Medicine.* 23:8. 2017.
5. Sunada, Y., Bernier, S. M., Utani, A., Yamada, Y., Campbell, K. P. *Human molecular genetics* 4:6. 1995.
6. Gawlik, K. I., Harandi, V. M., Cheong, R. Y., Petersen, A., Durbeej, M. *Matrix biology : journal of the International Society for Matrix Biology* 2018.
7. Gawlik, K. I., Li, J. Y., Petersen, A., Durbeej, M. *Human molecular genetics* 15:18. 2006.
8. Gawlik, K. I., Mayer, U., Blomberg, K., Sonnenberg, A., Ekblom, P., Durbeej, M. *FEBS letters* 580:7. 2006.
9. Gawlik, K. I., Akerlund, M., Carmignac, V., Elamaa, H., Durbeej, M. *PloS one* 5:7. 2010.
10. Gawlik, K. I., Durbeej, M. *Muscle & nerve* 42:1. 2010.
11. Maeder, M. L., Linder, S. J., Cascio, V. M., Fu, Y., Ho, Q. H., Joung, J. K. *Nature methods* 10:10. 2013.
12. Perez-Pinera, P., Kocak, D. D., Vockley, C. M., Adler, A. F., Kabadi, A. M., Polstein, L. R., Thakore, P. I., Glass, K. A., Ousterout, D. G., Leong, K. W., Guilak, F., Crawford, G. E., Reddy, T. E., Gersbach, C. A. *Nature methods* 10:10. 2013.
13. Gonzalez, S., Fernando, R. N., Perrin-Tricaud, C., Tricaud, N. *Nature protocols* 9:5. 2014.
14. Wojtal, D., Kemaladewi, D. U., Malam, Z., Abdullah, S., Wong, T. W., Hyatt, E., Baghestani, Z., Pereira, S., Stavropoulos, J., Mouly, V., Mamchaoui, K., Muntoni, F., Voit, T., Gonorazky, H. D., Dowling, J. J., Wilson, M. D., Mendoza-Londono, R., Ivakine, E. A., Cohn, R. D. *Am J Hum Genet* 98:1. 2016.

bioRxiv preprint doi: https://doi.org/10.1101/286500; this version posted March 23, 2018. The copyright holder for this preprint (which was not certified by peer review) is the author/funder, who has granted bioRxiv a license to display the preprint in perpetuity. It is made available under aCC-BY-NC-ND 4.0 International license.

15. Ran, F. A., Cong, L., Yan, W. X., Scott, D. A., Gootenberg, J. S., Kriz, A. J., Zetsche, B., Shalem, O., Wu, X., Makarova, K. S., Koonin, E. V., Sharp, P. A., Zhang, F. *Nature* 520:7546. 2015.
16. Esvelt, K. M., Mali, P., Braff, J. L., Moosburner, M., Yaung, S. J., Church, G. M. *Nature methods* 10:11. 2013.
17. Qi, L. S., Larson, M. H., Gilbert, L. A., Doudna, J. A., Weissman, J. S., Arkin, A. P., Lim, W. A. *Cell* 152:5. 2013.
18. Liao, H. K., Hatanaka, F., Araoka, T., Reddy, P., Wu, M. Z., Sui, Y., Yamauchi, T., Sakurai, M., O'Keefe, D. D., Nunez-Delicado, E., Guillen, P., Campistol, J. M., Wu, C. J., Lu, L. F., Esteban, C. R., Izpisua Belmonte, J. C. *Cell* 171:7. 2017.
19. Bonnemann, C. G., Wang, C. H., Quijano-Roy, S., Deconinck, N., Bertini, E., Ferreiro, A., Muntoni, F., Sewry, C., Beroud, C., Mathews, K. D., Moore, S. A., Bellini, J., Rutkowski, A., North, K. N., Members of International Standard of Care Committee for Congenital Muscular, D. *Neuromuscular disorders : NMD* 24:4. 2014.
20. Qiao, C., Li, J., Zhu, T., Draviam, R., Watkins, S., Ye, X., Chen, C., Li, J., Xiao, X. *Proceedings of the National Academy of Sciences of the United States of America* 102:34. 2005.
21. Bentzinger, C. F., Barzaghi, P., Lin, S., Ruegg, M. A. *FASEB journal : official publication of the Federation of American Societies for Experimental Biology* 19:8. 2005.
22. Qiao, C., Dai, Y., Nikolova, V. D., Jin, Q., Li, J., Xiao, B., Li, J., Moy, S. S., Xiao, X. *Molecular Therapy* 9:2018.
23. Meinen, S., Barzaghi, P., Lin, S., Lochmuller, H., Ruegg, M. A. *The Journal of cell biology* 176:7. 2007.
24. Reinhard, J. R., Lin, S., McKee, K. K., Meinen, S., Crosson, S. C., Sury, M., Hobbs, S., Maier, G., Yurchenco, P. D., Ruegg, M. A. *Science translational medicine* 9:396. 2017.
25. McKee, K. K., Crosson, S. C., Meinen, S., Reinhard, J. R., Ruegg, M. A., Yurchenco, P. D. *The Journal of clinical investigation* 127:3. 2017.
26. Hightower, R. M., Alexander, M. S. *Muscle & nerve* 57:1. 2018.
27. Rooney, J. E., Gurpur, P. B., Burkin, D. J. *Proceedings of the National Academy of Sciences of the United States of America* 106:19. 2009.
28. Perrin, A., Rousseau, J., Tremblay, J. P. *Molecular therapy. Nucleic acids* 6:2017.
29. Chen, J. S., Liu, J. C., Shen, L., Rau, K. M., Kuo, H. P., Li, Y. M., Shi, D., Lee, Y. C., Chang, K. J., Hung, M. C. *Cancer gene therapy* 11:11. 2004.
30. Thakore, P. I., D'Ippolito, A. M., Song, L., Safi, A., Shivakumar, N. K., Kabadi, A. M., Reddy, T. E., Crawford, G. E., Gersbach, C. A. *Nature methods* 12:12. 2015.
31. Lamar, K. M., Bogdanovich, S., Gardner, B. B., Gao, Q. Q., Miller, T., Earley, J. U., Hadhazy, M., Vo, A. H., Wren, L., Molkentin, J. D., McNally, E. M. *PLoS genetics* 12:5. 2016.
32. Quattrocelli, M., Capote, J., Ohiri, J. C., Warner, J. L., Vo, A. H., Earley, J. U., Hadhazy, M., Demonbreun, A. R., Spencer, M. J., McNally, E. M. *PLoS genetics* 13:10. 2017.
33. Kemaladewi, D. U., de Gorter, D. J., Aartsma-Rus, A., van Ommen, G. J., ten Dijke, P., t Hoen, P. A., Hoogaars, W. M. *FASEB journal : official publication of the Federation of American Societies for Experimental Biology* 26:4. 2012.

a

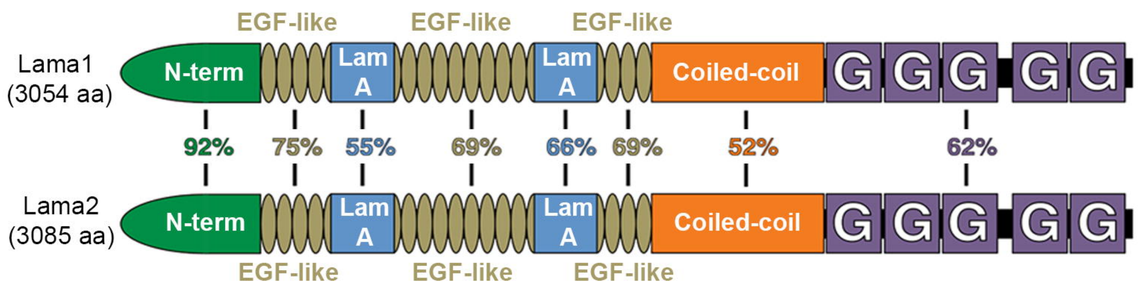

b

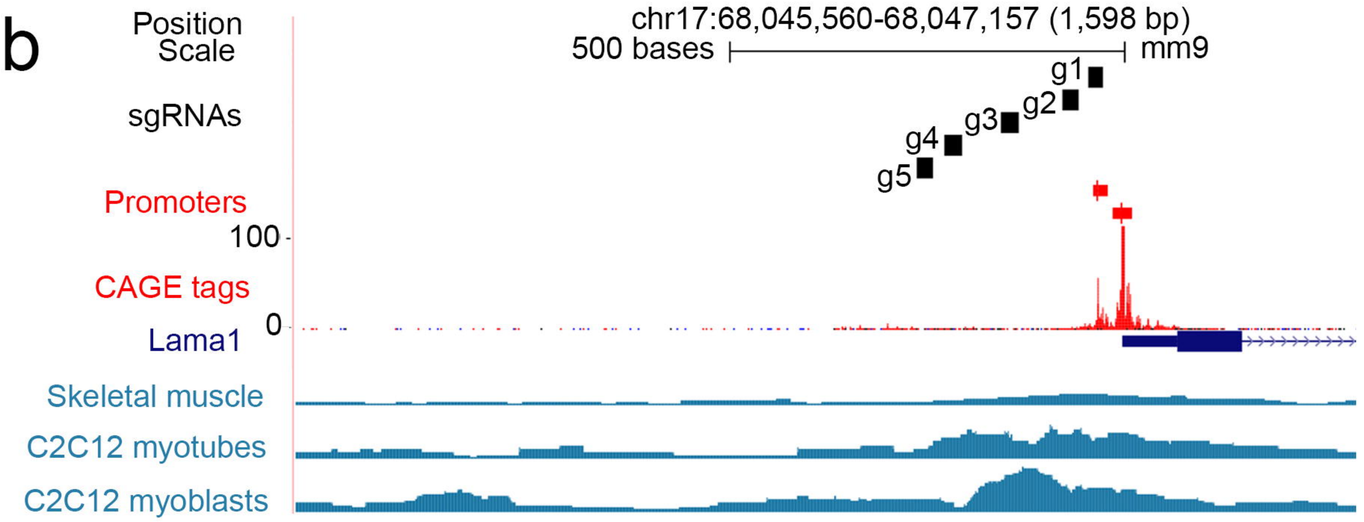

c

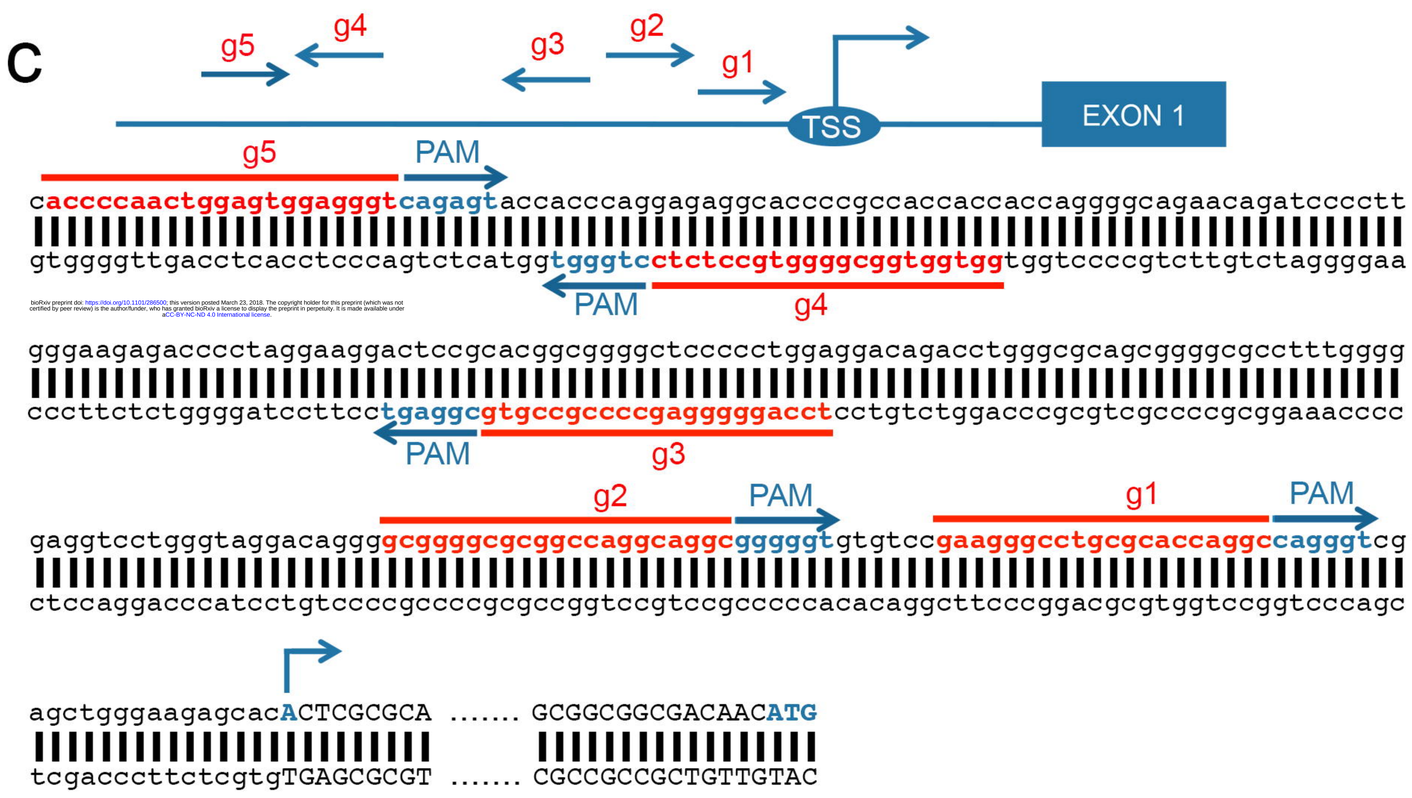

bioRxiv preprint doi: https://doi.org/10.1101/286500; this version posted March 23, 2018. The copyright holder for this preprint (which was not certified by peer review) is the author/funder, who has granted bioRxiv a license to display the preprint in perpetuity. It is made available under aCC-BY-NC-ND 4.0 International license.

d

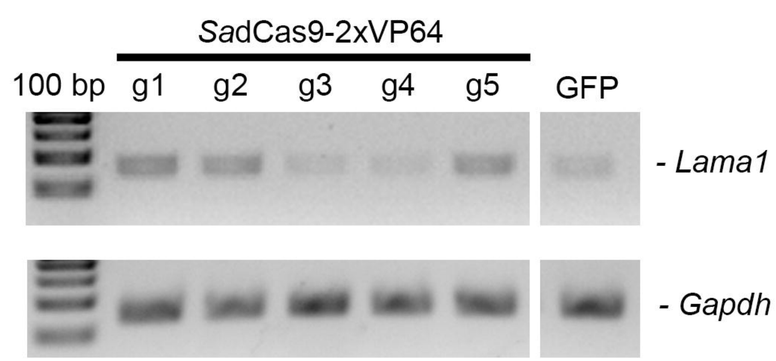

e

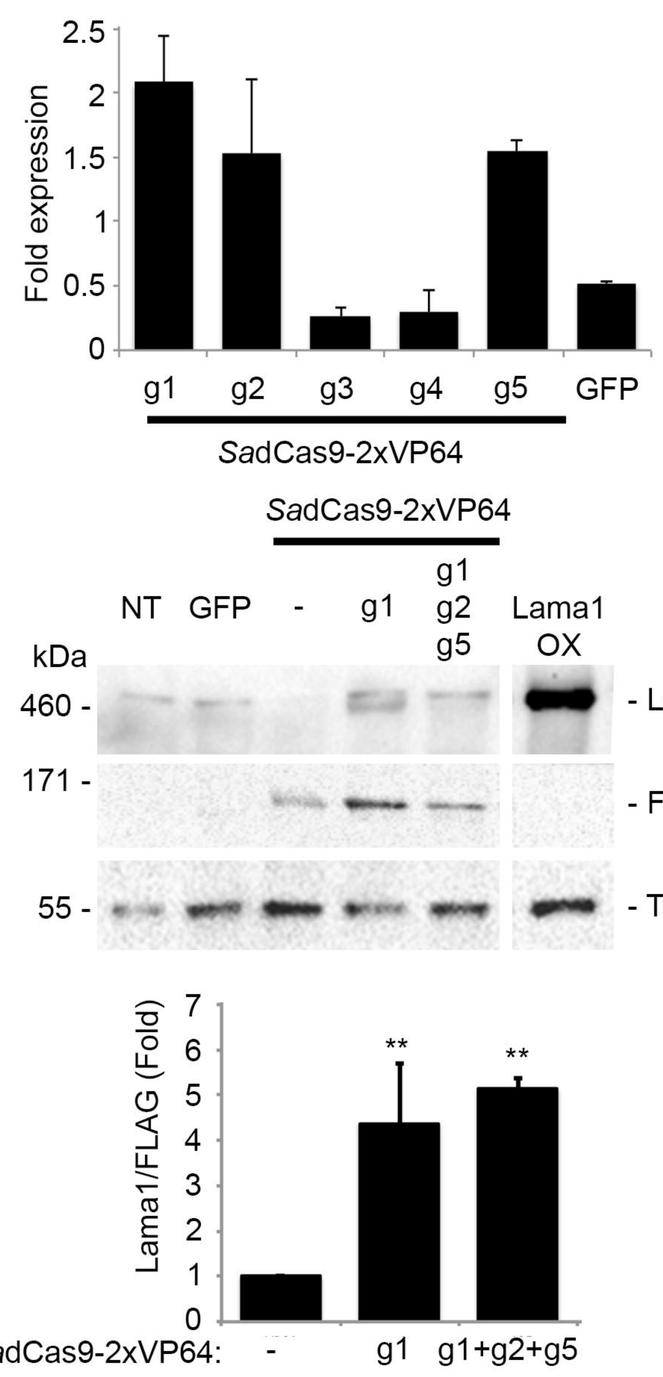

f

g

Figure 1

a

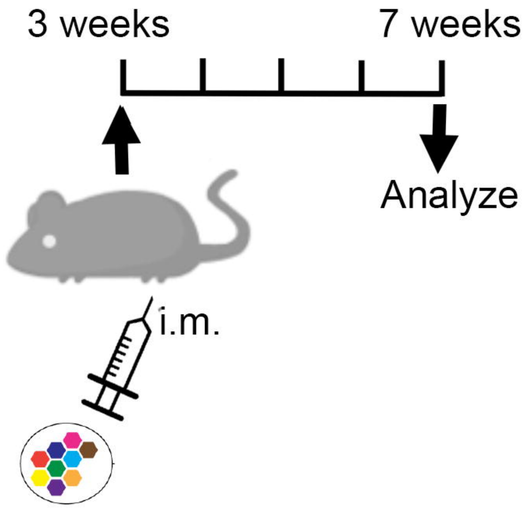
3 weeks
7 weeks
Analyze
i.m.

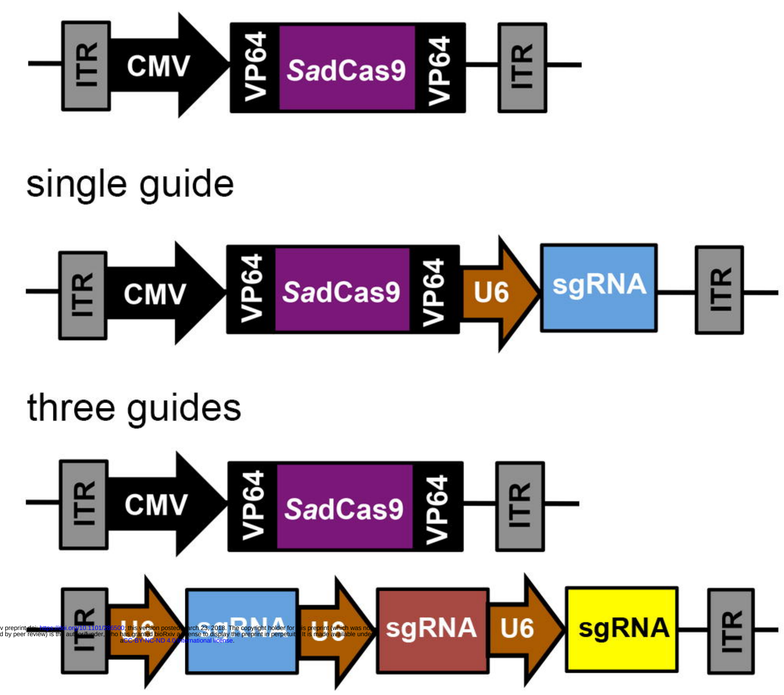
no guide
ITR
CMV
VP64
SadCas9
VP64
ITR
single guide
ITR
CMV
VP64
SadCas9
VP64
U6
sgRNA
ITR
three guides
ITR
CMV
VP64
SadCas9
VP64
ITR
ITR
U6
sgRNA
U6
sgRNA
U6
sgRNA
ITR

b

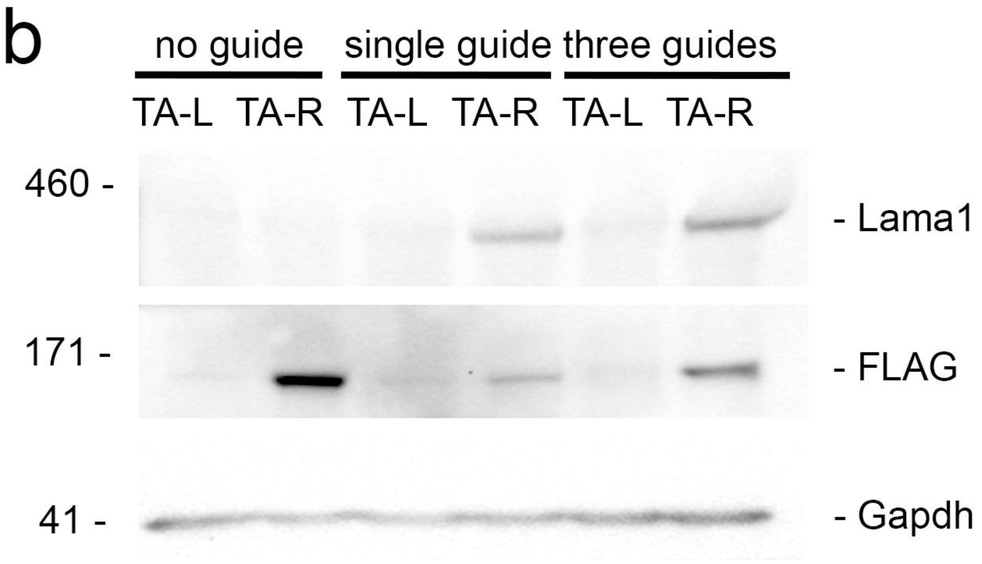
no guide
single guide
three guides
TA-L
TA-R
TA-L
TA-R
TA-L
TA-R
460 -
- Lama1
171 -
- FLAG
41 -
- Gapdh

c

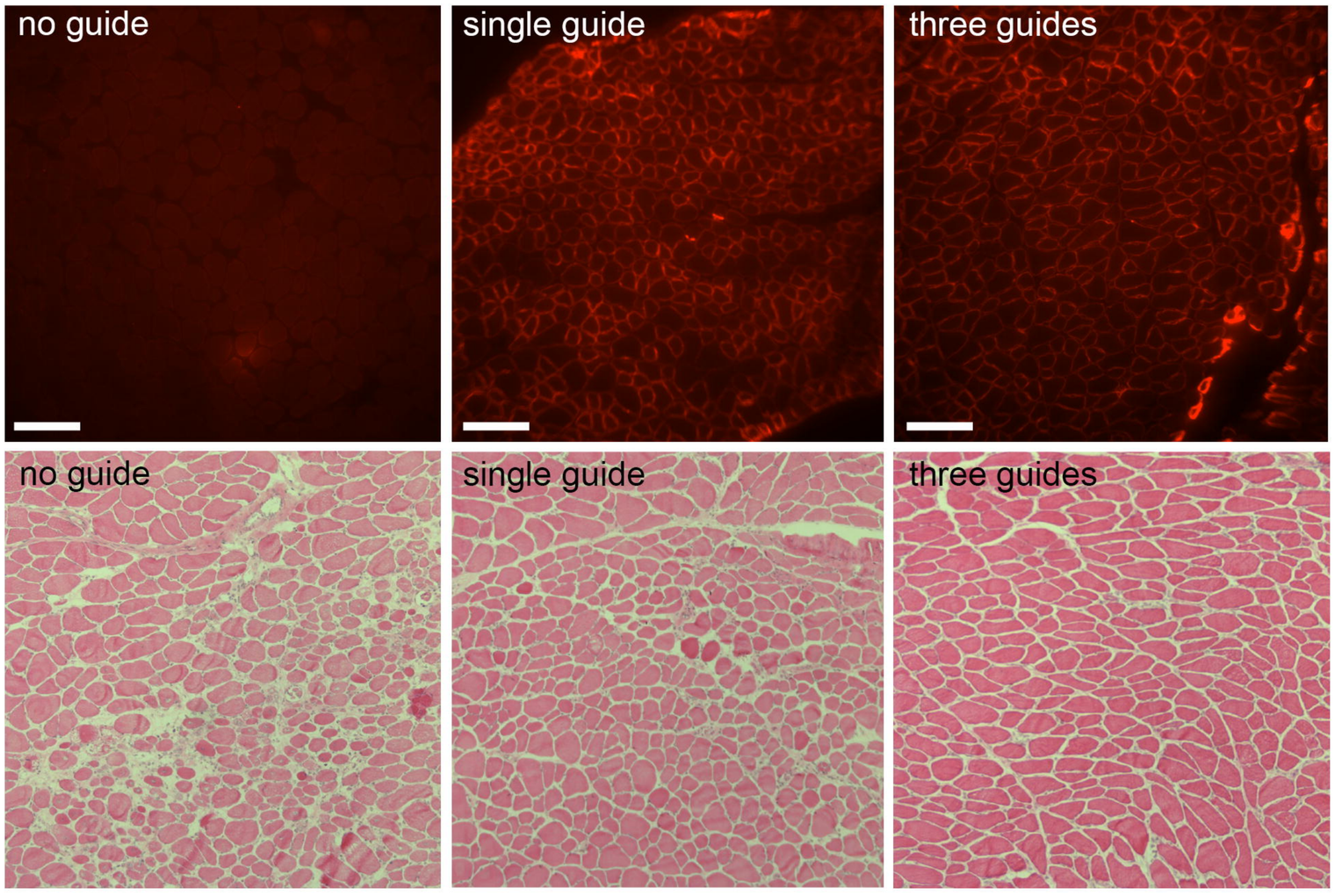
no guide
single guide
three guides
no guide
single guide
three guides

Figure 2

bioRxiv preprint doi: https://doi.org/10.1101/286500; this version posted March 23, 2018. The copyright holder for this preprint (which was not certified by peer review) is the author/funder, who has granted bioRxiv a license to display the preprint in perpetuity. It is made available under aCC-BY-NC-ND 4.0 International license.

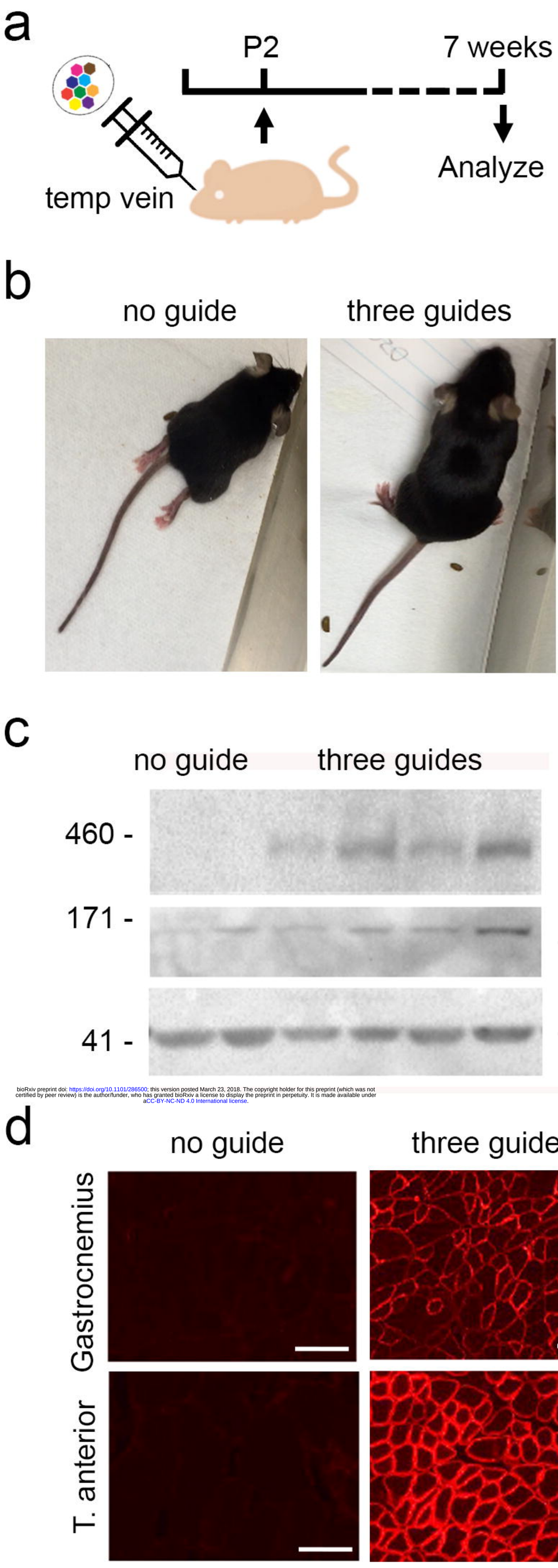

Figure 3

bioRxiv preprint doi: https://doi.org/10.1101/286500; this version posted March 23, 2018. The copyright holder for this preprint (which was not certified by peer review) is the author/funder, who has granted bioRxiv a license to display the preprint in perpetuity. It is made available under aCC-BY-NC-ND 4.0 International license.

Figure 4